Trans. Korean Soc. Noise Vib. Eng., 27(1) : 28~35, 2017
https://doi.org/10.5050/KSNVE.2017.27.1.028

한국소음진동공학회논문집 제 27 권 제 1 호, pp. 28~35, 2017
ISSN 1598-2785(Print), ISSN 2287-5476(Online)

A Numerical Study of New Vehicle Hydraulic Lift Activation by a Magneto-rheological Valve System for Precise Position Control

정밀 위치 제어를 위해 MR 밸브 시스템을 활용한 차량 유압 리프트에 대한 수치해석적 고찰

TaeHoon Lee*, Jhin-Ha Park*, Seung-Bok Choi†, Cheol-Soo Shin* and Ji-Young Choi**
이 태 훈 · 박 진 하 · 최 승 복 · 신 철 수 · 최 지 영

(Received September 1, 2016 ; Revised December 29, 2016 ; Accepted December 29, 2016)

Key Words : Hydraulic Vehicle Lift(유압 차량 리프트), Magneto-rheological Fluid(자기 유변 유체), Magneto-rheological Valve(자기 유변 밸브), Accurate Position Control(정밀 위치 제어), Hydraulic Valve System (유압 밸브 시스템)

ABSTRACT

Recently, conventional hydraulic car lift systems face the technological limitations due to a lack of height control. The demand for height controllability is required in many tasks such as wheel alignment, and requires compensation for the structural deformation of the lift caused by irregular load distribution. In order to resolve this limitation of the conventional car lift, in this work, a new type of a hydraulic vehicle lift using a magneto-rheological (MR) valve system is proposed and analyzed. Firstly, the dynamic model of vehicle lift is formulated to evaluate control performance; subsequently, an MR valve is designed to obtain the desired pressure drop required in the car lift. Next, a proportional-integral-derivative (PID) controller is formulated to achieve accurate control of the lifting height and then computer simulations are undertaken to show accurate height control performances of the proposed new car lift system.

요 약

최근 기존의 유압 차량 리프트는 높이제어의 어려움으로 인해 기술개발의 한계에 직면하였다. 휠 얼라이먼트나 차량의 하중 분포에 따른 미세한 불규칙적인 변형을 보상하기 위해서는 매우 정밀한 위치 제어성이 요구되고 있다. 이 연구에서는 이러한 기존 리프트 시스템의 한계를 해결하고자 매우 정교한 압력강하를 이끌어낼 수 있는 MR 밸브 시스템을 활용하여 새로운 차량 리프트를 제안하고 이에 대한 분석을 진행한다. 우선적으로 MR 밸브의 요구되는 성능을 파악하기 위해 유압 리프트의 운동방정식을 설립하고, 요구되는 압력강하를 얻기 위해 MR 밸브를 설계한다. 또한 정밀한 위치 제어 성능을 얻기 위해 PID 제어기를 설립하고, 시뮬레이션을 통해 제안된 시스템의 제어성을 검증한다.

† Corresponding Author; Member, Mechanical Engineering of Inha University
E-mail : seungbok@inha.ac.kr
* Member, Mechanical Engineering of Inha University
** Head of R&D Center, Heshbon Co., Ltd

‡ Recommended by Editor Jae Hung Han

1. Introduction

Due to the growth of automobile industry, the number of vehicles is continuously increasing with the number of used vehicles in the world already exceeding 1.2 billion[1]. For this reason, vehicle maintenance, service, and repair technologies have been greatly developed in the industry[2]. The hydraulic vehicle lift is one of the most widely used pieces of equipment for the repair and service of vehicles. However, because of the lack of precision control over this hydraulic system, the conventional lift system faces a technological limitation. This unrefined position control performance means that precise repair work, like a wheel alignment adjusting the angles of the wheels, cannot be performed well on the lift. Moreover, existing height controls cannot compensate easily the deformation of the structure caused from the irregular load distribution.

The MR fluid (MRF) consists of the micro-sized iron particles in a nonmagnetic fluid such as silicone oil. The rheological properties of MRF can be altered by an applied low power magnetic field. Based on this characteristic of MRF, various industry applications have been proposed for several years[3,4]. The MR valve in hydraulic systems, which can easily control the pressure drop of the hydraulic lines, is one such representative device[5~7]. From the previous research, the advantages of MR hydraulic valve systems can be defined as follows: (1) great controllability, (2) faster response, (3) lack of moving parts, (4) no mechanical complexity, (5) high power density, and (6) great durability. Consequently, the main contribution of this work is to propose a new type of hydraulic vehicle lift based on an MR hydraulic valve system to obtain precise position control performance. In order to achieve this goal, a mathematical model of the hydraulic vehicle lift is formulated to identify the required performance of the hydraulic MR valve system. Next, the control performance of the designed system is evaluated through a numerical analysis.

2. Dynamic Model

Figure 1 shows a rendering of the hydraulic vehicle lift and Fig. 2 shows the configuration of this hydraulic vehicle lift and presents the working principle of the system. The vehicle can be placed on the top table and its ascent can be performed by the hydraulic force of four MR cylinders. Each internal hydraulic cylinder pressure is controlled by the MR hydraulic valve system as shown in Fig. 3. In this figure, P_1 and P_3 are consistent output and input pressures, respectively,

Fig. 1 Rendering of MR valve activated vehicle lift

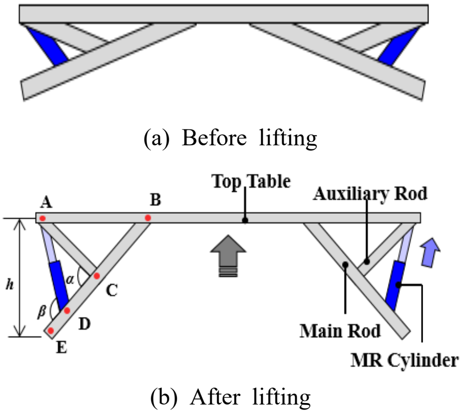

Fig. 2 Schematic of hydraulic vehicle lift

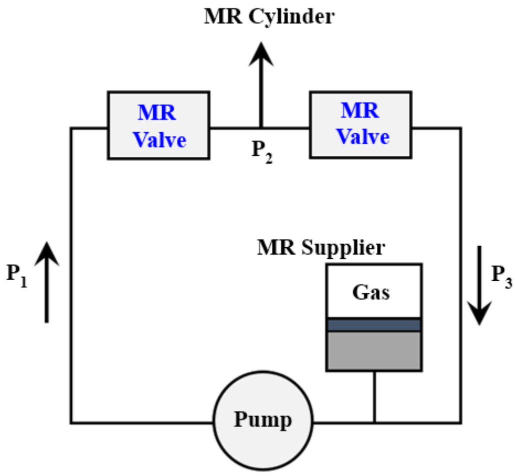

Fig. 3 Schematic of MR valve system

of the pump system. Through a pressure drop of MR valve 1, the desired P_2 can be obtained, and through the MR valve 2, a consistent P_3 can be maintained during steady state operation of the passive pump system.

In order to satisfy the objective of this work, a target specification of the vehicle lift can be defined as follows: (1) mass of lifted vehicle is less than 2000 kg, (2) controllable height range of top table is from 0.3 m to 1.9 m, and (3) accuracy of position control is ±0.5 mm.

Firstly, the governing equation of the lift motion should be derived to determine the required performance of the MR valve and evaluate the control performance of the hydraulic vehicle lift. In this work, m_{tp}, m_{mar}, and m_v are the mass of top table, main rod, and vehicle, respectively, with values of 420 kg, 170 kg, and 2000 kg, respectively. I_{mar}, the rotational moment of inertia of a main rod at Point E, is 286 kg·m^2. Figure 4(a) shows a free body diagram of top table for which the dynamic equation can be derived as follows:

$$2F_{Ay} + 2F_{By} - \frac{m_v}{2} g + m_{tp} g = \left(m_{tp} + \frac{m_v}{2} \right) \ddot{h}(t) \qquad (1)$$

Here, g is gravitational acceleration. Fig. 4(b) presents a free body diagram of joint A for

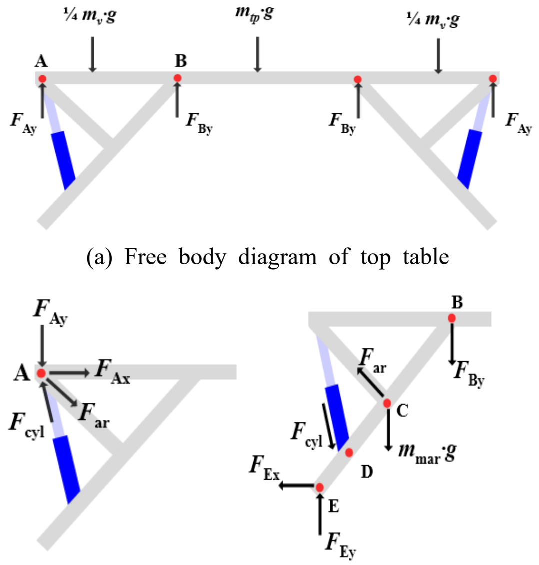

(a) Free body diagram of top table

(b) Free body diagram of joint A

(c) Free body diagram of main rod

Fig. 4 Free body diagram of the vehicle lift structure

which the dynamic equation can be derived as follows:

$$-F_{Ay} + F_{cyl} \sin\left(\beta - \frac{\alpha}{2} \right) - F_{ar} \sin\left(\frac{\alpha}{2} \right) = 0 \qquad (2)$$

$$F_{Ax} - F_{cyl} \cos\left(\beta - \frac{\alpha}{2} \right) + F_{ar} \cos\left(\frac{\alpha}{2} \right) = 0 \qquad (3)$$

A free body diagram of main rod can be presented as shown in Fig. 4(c), the dynamic equation of which can be derived as follows:

$$\begin{aligned} &(F_{By} - F_{Ey} + m_{mar} g)\sin\left(\frac{\alpha}{2} \right) + F_{Ex} \cos\left(\frac{\alpha}{2} \right) \\ &\quad - F_{cyl}\cos(\beta) + F_{ar}\cos(\alpha) = m_{mar} (\dot{\alpha}(t)/2)^2 L_{CE} \end{aligned} \qquad (4)$$

$$\begin{aligned} &(-F_{By} + F_{Ey} - m_{mar} g)\cos\left(\frac{\alpha}{2} \right) + F_{Ex} \sin\left(\frac{\alpha}{2} \right) \\ &\quad - F_{cyl}\sin(\beta) + F_{ar}\sin(\alpha) = m_{mar} (\ddot{\alpha}(t)/2) L_{CE} \end{aligned} \qquad (5)$$

$$\begin{aligned} &F_{By} \cos\left(\frac{\alpha}{2} \right) L_{BE} - F_{ar} \sin(\alpha) L_{CE} \\ &\quad + F_{cyl} \sin(\beta) L_{DE} = I_{mar} (\ddot{\alpha}(t)/2)) \end{aligned} \qquad (6)$$

Additionally, the relationship of the geometric variables can be defined as follows:

$$\alpha = 2\arcsin\left(\frac{h(t)}{2L_{CE}}\right) \tag{7}$$

$$\beta = \arccos\left(-\frac{k-\cos(\alpha)}{\sqrt{k^2-2k\cos(\alpha)+\cos^2(\alpha)+\sin^2(\alpha)}}\right) \tag{8}$$

Here, L_{CE}, L_{DE}, L_{BE}, and L_{CD} can be defined as 1.125 m, 0.9 m, 2.25 m, 0.225 m respectively. The value of k, defined by L_{CD}/L_{CE}, is 0.2. The force of the MR cylinder from P_2 can be presented as follow:

$$F_{cyl} = P_2 R_{cyl}^2 \pi \text{ where, } P_2 = P_1 - P_{MR1} \tag{9}$$

R_{cyl} is the radius of the MR cylinder piston and is 0.16 m. P_{MR1} is the pressure drop across the MR valve 1. The top table can be regarded as rigid body to simplify the problem and it can be identified that F_{Ay} is same with F_{By}.

Consequently, the nine unknown variables can be determined using the above equations.

3. MR Valve

Based on the derived dynamic equation, the required force of MR cylinder for the static equilibrium state of the lift can be derived as follows:

$$RF_{cyl}(t) = \frac{2gL_{CE}(m_v/2+m_{mar}+m_{tp})\sin(2D_1)}{(k-1)h(t)D_2+4L_{CE}\cos(D_1+D_3)\sin(2D_1)} \tag{10}$$

where,

$$D_1 = \operatorname{arccsc}\left(\frac{2L_{CE}}{h(t)}\right)$$

$$D_2 = \sqrt{\frac{-(h(t))^4+4L_{CE}^2(h(t))^2}{k\,L_{CE}^2(h(t))^2+(k-1)^2L_{CE}^4}}$$

$$D_3 = \arcsin\left(1-k-\frac{(h(t))^2}{2L_{CE}^2}\Big/\sqrt{(k-1)^2+\frac{(h(t))^2k}{L_{CE}^2}}\right)$$

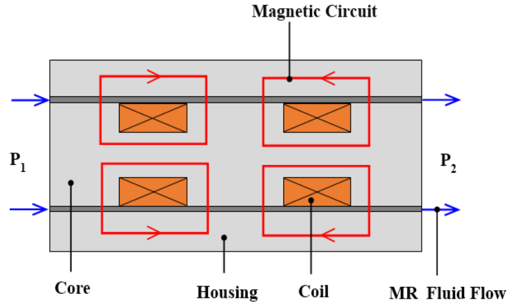

(a) Designation of component

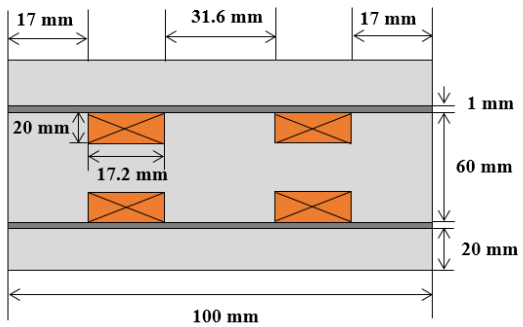

(b) Geometric parameter

Fig. 5 Schematic configuration of MR valve

A required pressure for the static equilibrium state can be calculated by Eq. (10). This pressure is increased by 6.81 MPa when the height of top table from ground, h, is minimized, while it is decreased by 1.46 MPa when h is maximized. Therefore, a controllable range of P_2 should exceed the range from 1.46 to 6.81 MPa to satisfy the target specification for a lift system and provide the desired dynamic motion. The configuration of the MR valve used in this work is presented as shown in Fig. 5. In addition, Fig. 5(b) shows the geometric parameter of MR valve. The coil is made of 300 turns of 23 AWG(American Wire Gauge) copper wire. The analytical pressure drop value of MR valve that is composed of two parts can be presented as follows[6]:

$$P_{MR1} = \Delta P_{viscous} + \Delta P_{yield} \tag{11}$$

$$\Delta P_{viscous} = \frac{6\eta QL}{\pi t_g^3 R} \tag{12}$$

$$\Delta P_{yield} = \frac{c_1\tau_1(B_1)L_1}{t_g} + 2\frac{c_2\tau_2(B_2)L_2}{t_g} \tag{13}$$

where,

$$c_i = 2.07 + \frac{12Q\eta}{12Q\eta + 0.8\pi R t_g^{\,2}\tau_i(B_i)}$$

$P_{viscous}$ presents the pressure drop due to the viscosity of the MR fluid. In this work, the commercially available MR fluid, MRF132DG from Lord Corporation, is used: its dynamic viscosity, η, is 0.112. The flow rate of MR fluid, Q, is 141 mL/s. Therefore, $P_{viscous}$ can be defined as 0.01 MPa. On the other hand, P_{yield} presents the pressure drop due to the yield stress of the MR fluid. τ_1 and τ_2 indicate the yield stress of MR fluid, which are caused by a magnetic flux density in the flow path of L_1 and L_2, respectively. B_1 and B_2 are the magnetic flux density in Tesla, which can be generated by current in a coil. As a material property of the commercial MR fluid MRF132DG, the relationship between the yield stress and magnetic flux density can be presented as follows[7]:

$$\begin{aligned}\tau_i(\text{kPa}) &= 52.962B_i^{\,4} - 176.51B_i^{\,3} \\ &\quad + 158.79B_i^{\,2} + 13.708B_i + 0.1442\end{aligned} \tag{14}$$

When the different currents are applied to the coil, the magnetic flux density in the flow path can be calculated from finite elements analysis as shown in Fig. 6. Based on this figure, τ_1 and τ_2 can be solved by Eq. (14). The total pressure drop of the MR valve by the different input current can be solved through the Eq. (11) as shown in Fig. 7. It can be identified that the pressure drop of MR valve is saturated at the 7.16 MPa by a current of about 1.25 A. The minimum pressure drop can be defined by 0.1 MPa when the current is not applied. Because P_2 can be expressed as $P_1 - P_{MR1}$, the suitable range of P_1 should be defined to exceed the required pressure range as follows:

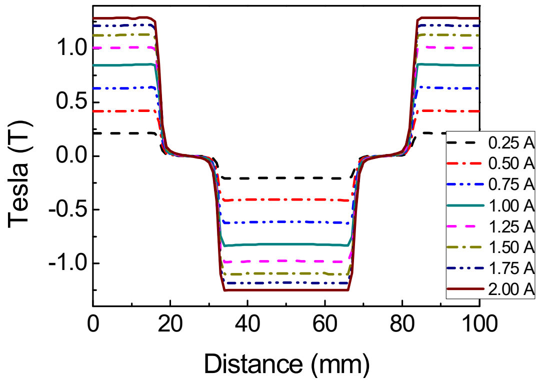

Fig. 6 Magnetic flux density in the flow path

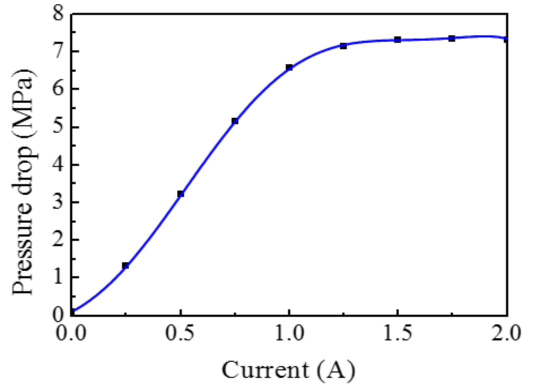

Fig. 7 Pressure drop of the MR valve

$$\begin{aligned}&6.81\ \text{MPa} \le P_1 - (P_{MR1})_{min} \\ &P_1 - (P_{MR1})_{max} \le 1.46\ \text{MPa}\end{aligned} \tag{15}$$

Therefore, the range of P_1 is identified as follows:

$$6.91\,\text{MPa} \le P_1 \le 8.62\,\text{MPa} \tag{16}$$

In order to provide the dynamic motion up and down with the same control algorithm, P_1 can be defined by the intermediate point in the range, 7.8 MPa. The constant input pressure of the pump, P_3, can be defined as follow:

$$\begin{aligned}&(P_2)_{min} - (P_{MR2})_{min} \ge (P_2)_{min} - P_{MR2} = P_3 \\ &(P_2)_{max} - (P_{MR2})_{max} \le (P_2)_{max} - P_{MR2} = P_3\end{aligned} \tag{17}$$

Therefore, it can be rewritten as follows:

$$P_1-(P_{MR1})_{max}-(P_{MR2})_{min}\geq P_3$$
$$P_1-(P_{MR1})_{min}-(P_{MR2})_{max}\leq P_3 \tag{18}$$

Because P_{MR1} is the same with P_{MR2}, can be determined by 0.54 MPa to satisfy Eq. (17) and (18).

4. Results and Discussions

The control input force of the MR cylinder can be defined based on the PID structure as follows:

$$F_{cyl}=RF_{cyl}(t)+p(dx-h(t)) + i\int(dx-h(t))dt+d(-\dot{h}(t)) \tag{19}$$

Where dx is the desired height of the top table and the control gains of p, d and i are chosen to be 8000, 25 000 and 1000 respectively to maintain the stable state. The control results in the time domain are presented in Fig. 8 and Fig. 9. Fig. 8(a) presents the position control response for the up motion when the top table is raised from its initial state, 0.3 m, to the desired height, 1.9 m. Fig. 8(b) shows the error between the actual and desired height of top table on a logarithmic scale. It is shown that the error is reduced by under the 0.5 mm target within 13.24 seconds. Fig. 8(c) shows the controlled pressure drop across the MR valve, which converges on the required pressure for the static equilibrium state of the top table while satisfying the workable pressure range of the valve system. Fig. 8(d) shows the input current value. Similarly, Fig. 9(a) presents the position control response for the down motion when the top table descends from initial state, 1.9 m, to the desired height, 0.3 m. It is shown that the distance error can be reduced by under the 0.5 mm target within 10.42 seconds with satisfying the workable pressure range of the valve system. Because of the existence of a small overshoot in the position control response, the distance error in Fig. 9(b) is increased for a few moments. Consequently, the target specification of the lift can be achieved by

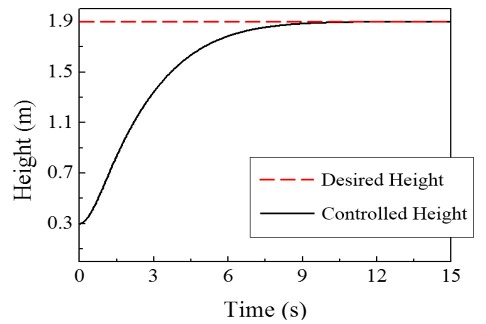

(a) Position control response

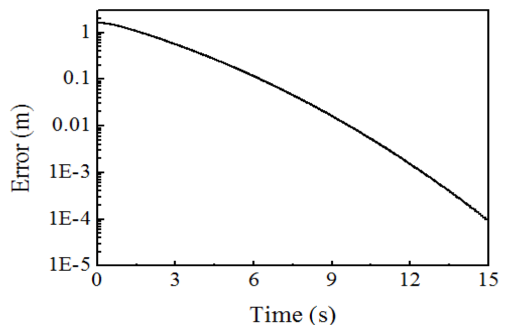

(b) Error between the height of top table and desired height

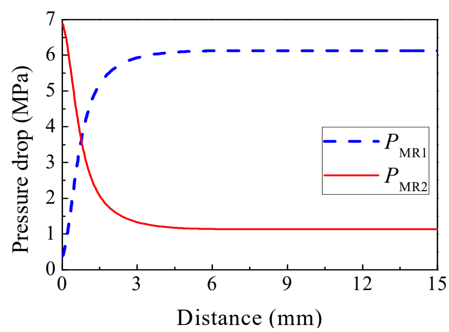

(c) Controlled pressure drop of MR valve

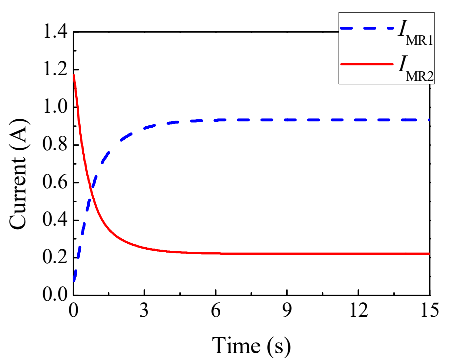

(d) Input current to coil

Fig. 8 Position control result for up motion

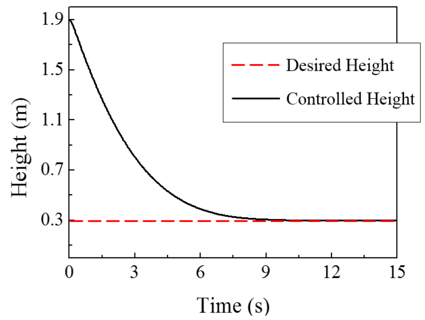

(a) Position control response

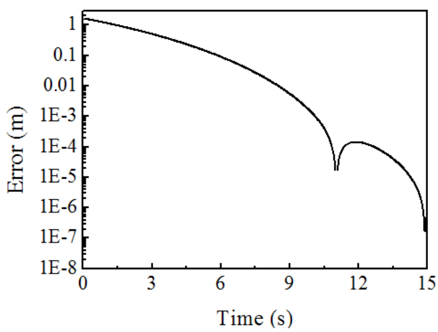

(b) Error between the height of top table and desired height

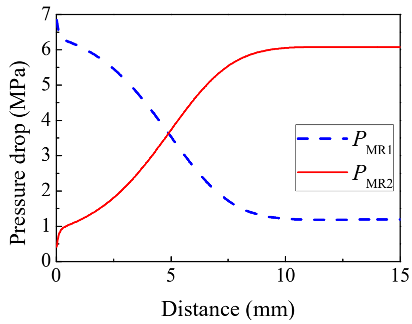

(c) Controlled pressure drop of MR valve

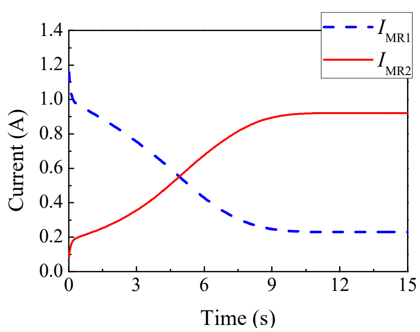

(d) Input current to coil

Fig. 9 Position control result for down motion the formulated control algorithm

5. Conclusion

In this work, a new type of hydraulic vehicle lift was proposed using the MR hydraulic valve system to obtain precise position control performance. The governing equations of motion were derived from the vehicle lift structure to identify the required performance of the hydraulic MR valve. The MR valve is designed to achieve a sufficient pressure drop for the control motion and the magnetic analysis is performed to obtain the relationship between the input current and pressure drop value based on the finite element method tool. Next, the evaluation of their control performances was performed by numerical simulation and it was shown that the proposed controllable system satisfies the required target specifications for the hydraulic vehicle lift. It is finally noted that the hardware test to verify the proposed system will be undertaken as a second phase of this work in the near future. In that experiment, a force sensor or pressure sensor will be used to eliminate the uncertainty of the system with respect to F_{Ay} and F_{By}.

Acknowledgments

This work was supported by the Small and Medium Business Administration (SMBA), grant funded by the Korea government (S2334760).

References

(1) Voelcker, J., 2014, 12 Billion Vehicles On World's Roads Now, 2 Billion By 2035: Report Green Car Reports Inc.

(2) Tom, D., 2012, Advanced Automotive Fault Diagnosis Routledge.

(3) Choi, S. B., Nam, M. H. and Lee, B. K., 2000, Vibration Control of a MR Seat Damper for Commercial Vehicles, Journal of Intelligent Material

Systems and Structures, Vol. 11, No. 12, pp. 936~944.

(4) Song, H. J., Woo, D. and Choi, S. B., 2006, Dynamic Characteristic Analysis of MR Impact Damper for Vehicle System, Transactions of the Korean Society for Noise and Vibration Engineering, Vol. 16, No. 7, pp. 754~761.

(5) Yoo, J, H. and Wereley, N, M., 2002, Design of a High-efficiency Magnetorheological Valve, Journal of Intelligent Material Systems and Structures, Vol. 13, No. 10, pp. 679~685.

(6) Ai, H. X., Wang, D. H. and Liao, W. H., 2006, Design and Modeling of a Magnetorheological Valve with Both Annular and Radial Flow Paths, Journal of Intelligent Material Systems and Structures, Vol. 17, No. 4, pp. 327~334.

(7) Nguyen, Q. H., Han, Y. M., Choi, S. B. and Wereley, N. M., 2007, Geometry Optimization of MR Valves Constrained in a Specific Volume Using the Finite Element Method, Smart Materials and Structures, Vol. 16, No. 6, pp. 2242~2252.

Seung-Bok Choi received the B.S. degree in Mechanical Engineering from Inha University in 1979, MS degree and Ph.D. degrees from Michigan State University in 1986 and 1990, respectively. He is currently Dean of the Graduate School and fellow professor in Inha University. He is a fellow of NAEK(National Academy Engineering of Korea), KAST(The Korean Academy of Science and Technology). His research interests are robust controller design and control of various systems using smart actuators.